Gümüşhane University Journal of Science and Technology

GUFBD / *GUJS* (2026) 16(3): 899-912 doi: 10.17714/gumusfenbil.1880379 Research Article

Impact of geometric imperfections on the optimal design of 3D steel frames

Osman TUNCA*

Karamanoğlu Mehmetbey University, Department of Civil Engineering, 72000, Karaman, Türkiye

• Received: 02.02.2026 • Accepted: 18.08.2026

Abstract

This study explores the impact of geometric imperfections on the optimal design of three-dimensional steel frames. The study employs a gaining-sharing knowledge-based algorithm (GSKA) integrated with ETABS through its Python programming language based open application programming interface (OAPI). This creates an automated design loop: GSKA proposes candidate designs, while Python scripts drive ETABS to perform structural analysis. Thus, the constraints against American Institute of Steel Construction-Load and Resistance Factor Design (AISC-LRFD) standards, including strength, stability, serviceability and constructability limits are verified. A three-dimensional two-story steel frame from an existing reference study serves as the benchmark structure for this investigation. The analysis evaluates the effect of geometric imperfections by considering three distinct structural models: a baseline geometrically perfect model, a model incorporating the code-prescribed geometric imperfection (ANSI/AISC), and a model with a double magnitude of imperfection. The automated API integration proved highly efficient, eliminating manual coding proses. The code-prescribed imperfections increase the optimal structural weight by approximately 7.80%, and doubled imperfections by up to 20.37%, demonstrating their critical influence on achieving safe and realistic optimal designs. The proposed GSKA -ETABS framework successfully leverages the synergy between a metaheuristic algorithm and commercial software automation. This approach provides a robust and efficient pathway for achieving material-efficient steel designs, balancing exploration and exploitation in the search for optimal solutions.

Keywords: Application programming interface, Finite element analysis, Gaining and shearing knowledge-based algorithm, Geometric imperfection, Steel space frame

1. Introduction

The relentless pursuit of material efficiency and structural safety in steel construction necessitates sophisticated design methodologies that can navigate complex, non-linear design spaces (Artar & Daloğlu, 2018). Optimal design of steel frames is a critical engineering challenge, aiming to minimize material consumption and cost while rigorously satisfying a multitude of design constraints related to strength, stability, serviceability, and constructability (Aydogdu et al., 2022). Traditional iterative design, heavily reliant on engineer intuition and manual calculations, often converges on feasible but suboptimal solutions. This has led to the growing adoption of structural optimization, a field dedicated to systematically finding the best possible design given a set of predefined objectives and constraints. In particular, size optimization of steel frames, which seeks the optimal cross-sectional dimensions for members, represents a direct and impactful application of this principle, with significant implications for economic and environmental sustainability (Tunca & Carbas, 2024). The complexity of this optimization problem is compounded by real-world structural imperfections. Among these, geometric imperfections—small, unavoidable deviations from the ideal geometry of a structure—are of paramount importance (Chan et al., 2025). These imperfections, arising from fabrication tolerances and erection processes, can induce second-order effects (P-Delta and P-delta), altering internal force distributions, reducing overall stability, and potentially leading to premature buckling (Zekavati et al., 2025). Consequently, modern design codes, such as the American Institute of Steel Construction-Load and Resistance Factor Design (AISC LRFD, 2001), mandate the explicit consideration of these imperfections in analysis, often through equivalent notional loads or initial sway configurations. However, the specific impact of varying imperfection magnitudes on the optimal design outcome—that is, on the final, most efficient member sizing—remains a nuanced area of investigation. Quantifying this impact is essential for developing designs that are not only theoretically optimal for a perfect model but also robust and safe under real-world conditions (Li & She, 2025).

*Osman TUNCA; osmantunca@kmu.edu.tr

ISSN: 2146-538X e-ISSN: 2146-538X https://dergipark.org.tr/tr/pub/gumusfenbil

To tackle this intricate optimization problems, researchers increasingly turn to metaheuristic algorithms (Tunca, 2022; Oğuzalp et al., 2025; Zekavati et al., 2025). These population-based search techniques, inspired by natural phenomena, are well-suited for global exploration of discontinuous and non-convex design spaces typical in structural engineering. The Gaining-Sharing Knowledge-Based Algorithm (GSKA) is one such contemporary metaheuristic, which emulates the process of knowledge acquisition and sharing across different stages of life (Mohamed et al., 2020). Its mechanism balances exploration (diversifying the search) and exploitation (refining good solutions), making it a promising tool for structural optimization. Despite their power, a significant practical barrier to applying metaheuristics like GSKA to real-world frames has been the integration with high-fidelity structural analysis. While standalone optimization code can handle simplified models, it often lacks the robust analysis engines required for professional design (Tunca, 2025; Tunca & Carbas, 2026). This gap is bridged by leveraging the advanced capabilities of modern commercial finite element analysis (FEA) software, such as ETABS, which is an industry standard for building analysis and design (ETABS, 2008; Bora & Türkay, 2025). Crucially, ETABS provides an Open Application Programming Interface (OAPI) accessible via the Python programming language. This interface enables external software to programmatically control ETABS—creating models, running analyses, extracting results, and checking design codes. The integration of a metaheuristic optimizer with a commercial FEA platform through such an API creates a powerful, automated design loop. The optimizer proposes candidate designs (member sizes), which are then analysed and evaluated for constraint adherence within the high-fidelity FEA environment, with feedback guiding the next iteration of the search (Erdem Çerçevik et al., 2021; Prayogo et al., 2024).

This study presents a comprehensive investigation that merges these advanced computational strands. Its primary objective is to rigorously quantify the effect of codified and amplified geometric imperfections on the optimal design of three-dimensional steel frames. The research employs a novel computational framework that seamlessly integrates the GSKA metaheuristic with ETABS via its Python-based OAPI. This automated framework is applied to a benchmark three-dimensional, two-story steel frame adopted from the literature (Artar & Daloğlu, 2018). Then, the mentioned reference optimization problem solved via GSKA by Tunca in 2025 (Tunca, 2025). In this study, three distinct structural models are optimized and compared: a baseline model with no imperfections (same with original reference study), a model incorporating the standard geometric imperfection prescribed by American National Standards Institute / American Institute of Steel Construction (ANSI/AISC, 2022), and a model with a doubled imperfection magnitude to assess sensitivity. The performance of the GSKA-ETABS integration is evaluated for its computational efficiency and effectiveness in handling the automated design cycle. The findings of this study aim to provide clear insights into the significance of imperfection modelling in optimization, demonstrate the practical utility of coupling metaheuristics with commercial software automation, and offer engineers a robust, automated pathway for achieving material-efficient, code-compliant steel designs that account for real-world structural uncertainties.

The general structure of this study is as follows: the general idea, main goal, and innovative aspect are described in the first section; the methodology of the study is examined from the second through the fifth sections; the design examples and their thorough justifications are included in the sixth section; and the outcomes are embraced in this section. Ultimately, the seventh and the eighth sections provide the study's discussion of the principal results and highlighting the concluding remarks, respectively.

2. Mathematical model for 3D steel frames

The present study addresses the discrete optimum design of steel frames under strength, serviceability, and geometric constraints, with the objective of minimizing the total structural weight. The design variables consist of integer values corresponding to standard steel section profiles, organized into member groups for practical fabrication. Formally, the optimization seeks an integer vector I:

$$I^T = [I_1 \quad I_2 \quad \dots \quad I_{ng}] \tag{1}$$

where I_i represents the index of the selected steel section for member group i, and ng is the total number of design groups. The objective function to be minimized is the total weight (W) of the frame:

$$W = \sum_{i=1}^{ng} \gamma_i A_i \sum_{j=1}^{nmg} l_j \tag{2}$$

Here, γ_i and A_i denote the unit weight and cross-sectional area of the chosen profile for group i, respectively, nmg is the number of members in group i, and l_j is the length of member j within that group.

In this study, American Institute of Steel Construction-Load and Resistance Factor Design (AISC-LRFD) is considered. The design must satisfy the following constraints:

●Top-story drift constraint:

$$\Delta_t \leq \Delta_{t-max} \tag{3}$$

where Δ_t is the lateral top displacement, and Δ_{t-max} is the allowable top drift.

●Inter-story drift constraint:

$$\frac{\Delta_j - \Delta_{j-1}}{h_j} \leq \delta_{max} \quad j = 1,2,\dots,ns \tag{4}$$

where Δ_j is the lateral displacement at story j, h_j is the storey height, δ_{max} is the allowable drift ratio, and ns is the number of stories.

●Displacement constraints:

$$d_i \leq d_{max} \quad i = 1,2,\dots,ncd \tag{5}$$

where d_i is a displacement component (e.g., beam deflection), d_{max} is its allowable limit, and ncd is the number of controlled displacements. For beams, the limit is typically span/300, while for columns under service loads, the limit is height/300.

●Shear capacity constraint for beam-column members:

$$V_u \leq \varphi_v V_n \quad i = 1,2,\dots,ncd \tag{6}$$

in which V_u is the required shear strength, V_n is the nominal shear strength, and φ_v is the shear resistance factor.

●Combined axial-flexural strength constraint (interaction equation):

$$\begin{aligned} &\frac{P_u}{\varphi_c P_n} + \frac{8}{9}\left(\frac{M_{ux}}{\varphi_b M_{nx}} + \frac{M_{uy}}{\varphi_b M_{ny}}\right) \leq 1 \ \leftarrow \frac{P_u}{\varphi_c P_n} \geq 0.2 \\ &\frac{P_u}{2\varphi_c P_n} + \left(\frac{M_{ux}}{\varphi_b M_{nx}} + \frac{M_{uy}}{\varphi_b M_{ny}}\right) \leq 1 \ \leftarrow \frac{P_u}{\varphi_c P_n} < 0.2 \end{aligned} \tag{7}$$

where P_u is the required axial strength; M_{ux} and M_{uy} are the required flexural strengths about the principal x and y axes, respectively; P_n, M_{nx}, and M_{ny} are the corresponding nominal strengths; and φ_c and φ_b are the resistance factors for compression and bending. For members in tension, $\varphi_c P_n$ is replaced by the design tensile strength $\varphi_t P_n$.

●Flange width compatibility at beam-column joints:

For connections of beams aligned with the global X-axis (bending about the column's minor y axis), the flange width of the beam must not exceed the flange width of the column:

$$B_{f_{X,beam}} \leq B_{f,column} \quad j = 1,2,\dots,nj \tag{8}$$

For connections of beams aligned with the global y axis (bending about the column's major x axis), the flange width of the beam must not exceed the clear depth of the column web, approximated here conservatively as the overall depth of the column section to avoid complex connection details:

$$B_{f_Y,beam} \leq D_{column} \quad j = 1,2, \ldots, nj \tag{9}$$

Here, $B_{f_X,beam}$ and $B_{f_Y,beam}$ are the flange widths of beams framing into the joint in the x and y directions, respectively; $B_{f,column}$ and D_{column} are the flange width and overall depth of the column section at that joint. These constraints prevent physical interference and ensure that standard connection details can be applied, maintaining the practicality of the optimized designs.

●Column continuity constraints over adjacent stories:

$$D_{column,s} \leq D_{column,\ s-1} \quad s = 1,2, \ldots, nu \tag{10}$$

$$M_{column,s} \leq M_{column\ ,s-1} \quad s = 1,2, \ldots, nu \tag{11}$$

where $D_{column,s}$ and $M_{column,s}$ represent the depth and mass per unit length of the column section at storey s. These constraints maintain architectural alignment and load transfer consistency, with nu being the number of such continuity conditions.

The optimization problem is therefore a constrained, integer nonlinear programming formulation. The challenge lies in efficiently navigating the discrete search space of standard steel sections and satisfying the complex, interdependent constraints imposed by requirements relating to strength, stability, serviceability and detailing.

2.1. Modelling global geometric imperfection in three-dimensional steel frames

The influence of geometric imperfections on the global stability and optimum design of three-dimensional steel frames is explicitly considered in this study in accordance with the provisions of the American National Standards Institute / American Institute of Steel Construction (ANSI/AISC, 2022). For the accurate stability analysis of three-dimensional steel moment frames, the structural model must account for the effects of global geometric imperfections such as initial out of plumbness and nodal position deviations. These imperfections are represented in the analysis by applying a system of equivalent horizontal forces, commonly referred to as notional loads, to the structure in its original undeformed configuration. This modeling approach simulates a small initial lateral sway and is essential for capturing second order effects, particularly in asymmetric or irregular three-dimensional structures. The notional forces are applied independently along each of the two principal horizontal axes to accurately evaluate the most critical stability demands on the frame in all directions.

The magnitude of the notional force at each floor level is determined based on the total vertical load acting on that story. A standard imperfection ratio of 1/500, corresponding to an angle of 0.002 radians, is used. The horizontal force for a given level i is therefore calculated using the expression

$$H_i = 0.002\ G_i \tag{12}$$

In equation 12, G_i is the total factored vertical load at that story. In practical application using Load and Resistance Factor Design, the full factored gravity load is applied. When using Allowable Stress Design methodologies, the vertical load is first increased by a factor of 1.6 before applying the 0.002 coefficient. These forces are then distributed proportionally to individual column nodes based on the share of the vertical load each column supports. The direction of force application is chosen to produce the most unfavorable structural response, and the analysis is conducted separately for both positive and negative directions along each primary axis to ensure all potential critical loading scenarios are comprehensively assessed. In the implementation within ETABS, the notional loads are introduced as independent static load cases. For each story, the horizontal force is calculated by equation 12 is distributed to the column nodes in proportion to the vertical load carried by each column. The notional loads are applied separately in the positive and negative global x and y directions to capture the most critical sway response. These load cases are then combined with the gravity according to the AISC-LRFD load combination requirements, ensuring that the effects of geometric imperfections are properly considered in all design evaluations. In ETABS, the stiffness modification factor τ_b (Tau-b) is used within the AISC 360 Direct Analysis Method (DAM) to reduce the flexural stiffness of members that contribute to the lateral stability of the structure, so that the finite element models more realistically reflect inelastic and geometric imperfection effects.

In ETABS, the stiffness modification factor τ-b (tau-b) is used within the AISC 360 Direct Analysis Method (DAM) to reduce the flexural stiffness of members that contribute to the lateral stability of the structure, so that the "perfect" (undamaged) model more realistically reflects inelastic and geometric imperfection effects.

3.Gaining-sharing knowledge-based algorithm

The gaining-sharing knowledge-based algorithm (GSKA), proposed by Mohamed et al. (2020), is a novel population-based metaheuristic inspired by the process of human social learning and cognitive development throughout a lifespan (Mohamed et al., 2020). Diverging from common biological or physical metaphors, GSKA models the fundamental mechanism of how individuals acquire (gain) and disseminate (share) knowledge. This process naturally transitions from a broad, exploratory learning phase in youth to a focused, experience-driven knowledge exchange in maturity. The algorithm is designed to mathematically formalize this transition to effectively balance exploration (diversifying the search) and exploitation (intensifying the search in promising regions). GSKA operates through two distinct sequential phases, with a dynamic internal mechanism controlling the shift between them.

a) The Experience Equation and Phase Transition Mechanism

The adaptive behavior of GSKA is governed by the experience equation, which determines the number of decision variables (dimensions, D) processed by each phase in a given generation (G). This is controlled by the knowledge rate parameter ($k > 0$), regulating the transition speed.

The number of dimensions updated in the Junior Phase, D_{junior}, decreases nonlinearly over generations:

$$D_{junior}(G) = D \times (1 - G/GEN)^k \quad (13)$$

where D is the total problem dimensionality, and GEN is the maximum number of generations.

Consequently, the number of dimensions updated in the Senior Phase, D_{senior}, increases complementarily:

$$D_{senior}(G) = D - D_{junior}(G) \quad (14)$$

For $k = 1$, the transition is linear. For $0 < k < 1$, the junior phase dominates for a longer period, emphasizing prolonged exploration. For $k > 1$, the transition to the senior phase is rapid, favoring earlier exploitation.

b) Junior Gaining-Sharing Phase (Exploration)

This phase simulates early-life learning. An individual x_i gains knowledge from its immediate, trusted network—modeled as the nearest better (x_{i-1}) and nearest worse (x_{i+1}) individuals in the current sorted population. Concurrently, driven by curiosity, it shares knowledge with a randomly selected individual x_r from the entire population.

For each dimension j to be updated, the rule is applied with a probability defined by the knowledge ratio k_r. The update rule is:

$$\begin{aligned}
&if\ rand(0,1) \leq k_r then \\
&if\ f(x_i) > f(x_r) \rightarrow x_{ij}^{new} = x_{ij} + k_f \times \left[\left(x_{(i-1)j} - x_{(i+1)j}\right) + \left(x_{rj} - x_{ij}\right)\right] \\
&otherwise \qquad \rightarrow x_{ij}^{new} = x_{ij} + k_f \times \left[\left(x_{(i-1)j} - x_{(i+1)j}\right) + \left(x_{ij} - x_{rj}\right)\right]
\end{aligned} \tag{15}$$

Here, k_f (knowledge factor) scales the overall influence of the gained and shared knowledge. The condition based on the fitness f(x) determines the direction of the "sharing" component.

c) Senior Gaining-Sharing Phase (Exploitation)

This phase models the experienced stage. The population is sorted and divided into three groups: the best individuals (top p%), the worst individuals (bottom p%), and the middle individuals. An individual x_i strategically gains knowledge by learning from the success of the best group and avoiding the poor performance of the worst group, while sharing knowledge with a randomly selected middle-group individual x_m.

The update rule for a dimension j in this phase is:

$$\begin{aligned}
&if\ rand(0,1) \leq k_r\ then \\
&if\ f(x_i) > f(x_m) \rightarrow x_{ij}^{new} = x_{ij} + k_f \times \left[\left(x_{best,r1,j} - x_{worst,r2,j}\right) + \left(x_{mj} - x_{ij}\right)\right] \\
&otherwise \qquad \rightarrow x_{ij}^{new} = x_{ij} + k_f \times \left[\left(x_{best,r1,j} - x_{worst,r2,j}\right) + \left(x_{ij} - x_{mj}\right)\right]
\end{aligned} \tag{16}$$

Here, $x_{best,r1}$ and $x_{worst,r2}$ are individuals randomly selected from the best and worst groups, respectively. x_m is randomly selected from the middle group. The detailed pseudocode of GSKA is given in Algorithm 1.

Algorithm 1. The pseudocode of GSKA.

1. $Initialize\ GSKA\ Parameters$:
   $NP(populationsize), k_f, k_r, k, p, GEN.$
2. $Randomly\ initialize\ the\ population$:
   $X\_i\ (i\ =\ 1, \dots, NP).$
3. $Evaluate\ the\ fitness\ f(X_i) for\ each\ individual.$
4. $For\ generation\ G\ =\ 1\ to\ GEN$:
   $a.$ $\boldsymbol{Apply\ the\ Experience\ Equation}$:
   $D_junior = floor(D * (1 - G/GEN)^k)$
   $D_senior = D - D_junior$
   $b.$ $\boldsymbol{Junior\ Phase}$:
   $Sort\ the\ population\ in\ ascending\ order\ of\ fitness.$
      $For\ i\ =\ 1\ to\ NP$:
         $Forj = 1\ to\ D_{junior}$:
            $operate\ Eq.(14)$
         $End\ For\ (j)$
      $End\ For\ (i)$
   $c.$ $\boldsymbol{Senior\ Phase}$:
   $Sort\ the\ population\ and\ categorize\ into\ groups$
   $(Bestp\%, Worstp\%, Middle(100 - 2p)\%).$
      $For\ i\ =\ 1\ to\ NP$:
         $For\ j = \left(D_{junior+1}\right)\ to\ D: //Seniordimensions$
            $operate\ Eq.(15)$
         $End\ For\ (j)$
      $End\ For\ (i)$
   $Evaluate\ new\ candidate\ solutions\ \left(f(X_{new}[i])\right).$
   $If\ f(X_{new}[i]) \leq f(X_i)\ , then\ X_i = X_{new}[i].$
      $Update\ the\ global\ best\ solution\ if\ improved.$
5. $Return\ the\ Global\ Best\ Solution.$

GSKA is a powerful optimizer characterized by its intuitive human-learning metaphor, a structured two-phase architecture (Junior and Senior), and an intelligent transition mechanism governed by the experience equation ($D_{junior/senior}$). This architecture facilitates an effective balance between exploration and exploitation in complex search spaces.

4. Integration of ETABS with python via open application programming interface (OAPI)

The structural optimization process for steel design necessitates a robust and automated interface between the optimization algorithm and the structural analysis engine. In this study, this critical link was established by leveraging the open application programming interface (OAPI) of ETABS, a widely-used structural analysis software (Bora & Türkay, 2025). The OAPI allows for bidirectional, programmatic communication with ETABS from an external environment. Using Python as the control language, the optimization algorithm (e.g., GSKA) is scripted to automatically generate the structural model in ETABS by defining materials, sections, nodal coordinates, member assignments, loads, and load cases. Subsequently, the API commands are used to initiate the analysis and retrieve key structural response data, such as member forces, nodal displacements, and stress ratios. This extracted performance data is then passed back to the Python-based optimization script to calculate the objective function (e.g., total weight) and evaluate constraint violations (e.g., code compliance checks). This seamless integration creates a closed-loop workflow where the optimizer iteratively proposes new design variable sets (e.g., cross-sectional properties), and the ETABS-Python interface performs the corresponding analysis and feedback without manual intervention, enabling efficient and high-fidelity evaluation of thousands of candidate designs. The automation steps of GSKA with Python are described in Algorithm 2.

Algorithm 2. Pseudocode for OAPI

1. *Initialize ETABS application via API from Python.*
2. *Create new ETABS model or open existing template.*
3. *For each optimization iteration:*
   a. *Receivedesignvariables(e.g., sectionsizes) from the optimizer (GSKA).*
   b. *Use ETABS API to:*
      i. *Assign new section properties to corresponding frame elements.*
      ii. *Update load patterns or magnitudes if part of optimization.*
      iii. *Run the analysis.*
   c. *Use ETABS API to extract results:*
      i. *Get frame forces.*
      ii. *Get joint displacements.*
      iii. *Get design outputs.*
   d. *In Python, process the extracted results:*
      i. *Calculate the objective function.*
      ii. *Evaluate constraints.*
      iii. *Pass the fitness value (objective and penalty) back to the optimizer.*
   e. *The optimizer generates a new set of design variables for the next iteration.*
4. *After optimization loop finishes, use API to save the final optimal model.*
5. *Close the ETABS application.*

5. Problem definitions

The primary original benchmark is the 16-member steel space frame, previously studied by Artar and Daloğlu in 2018 (Artar & Daloğlu, 2018). The benchmark structure is a 1-bay × 1-bay, 2-story steel space frame with a bay width of 5.5 m in two direction and a story height of 3.6 m. In their study, the steel space frame structure is subjected to a uniformly distributed gravity load of 20 kN/m on all beams and a lateral wind load of 40 kN applied at the top level, with displacement limits set to 1.8 cm for the top story drift and 0.9 cm for the inter-story drift. Three member groups of the mentioned steel space frame are illustrated in Figure 1. Three member groups are defined: Group 1 comprises the corner columns, Group 2 comprises the beams in x-directions, and Group 3 comprises the beams in y direction, as illustrated in Figure 1. The member sections are selected from a discrete design pool of 64 standard W profiles (W8X15, W8X21, W8X24, W8X28, W8X31, W8X35, W8X40, W10X15, W10X22,W10X26, W10X33, W10X39, W10X54, W10X77, W12X19, W12X26, W12X30, W12X35, W12X40, W12X45, W12X50, W12X53, W12X58, W12X72, W12X96, W14X26, W14X30, W14X34, W14X38, W14X43, W14X48, W14X53, W14X61, W14X68, W14X74, W14X82, W14X90, W14X120, W16X26, W16X31, W16X36, W16X40, W18X35, W18X40, W18X50, W18X76, W21X50, W21X62, W21X132, W24X68, W24X103, W27X94, W27X161, W30X108, W30X148, W30X191, W33X221, W36X150, W36X170 W, W36X182, W36X194, W40X149, W40X167, W40X183). Then, the same frame design problem was optimized utilizing GSKA without considering initial geometric imperfections by Tunca (Tunca, 2025). The handled geometrically perfect steel frame optimization problem by Tunca is considered as CASE-0 for this study.

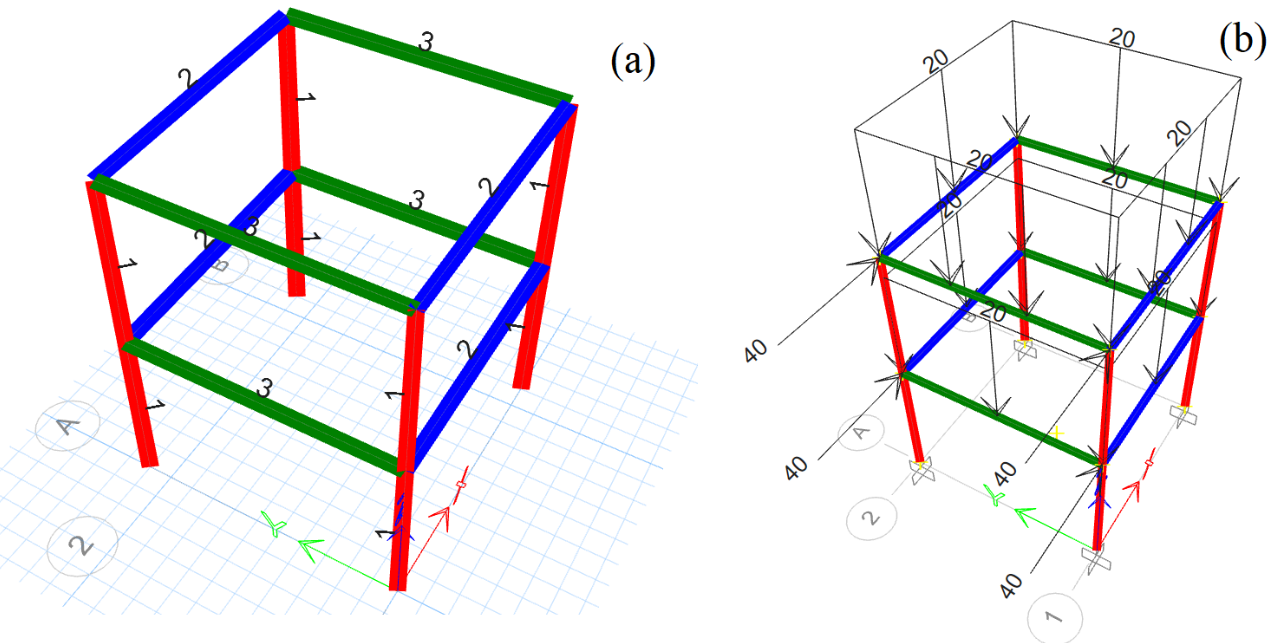

Figure 1. 16-member steel space frame (Artar & Daloğlu, 2018). (a) Group distribution in structural elements. (b) Load and support conditions

In this study, to investigate the influence of structural imperfections, two additional cases are introduced. The second and third cases (CASE-1 and CASE-2) use the same 16-member frame and now incorporate geometric imperfections. In addition to the code-prescribed imperfection magnitude of 0.2% (CASE-1), CASE-2 employs a doubled imperfection ratio of 0.4% to evaluate the sensitivity of the optimal design to deviations beyond typical fabrication tolerances. Such larger imperfections may arise from construction inaccuracies, differential foundation settlements, or unusual erection sequences. This scenario demonstrates the potential consequences of underestimating geometric imperfections and highlights the importance of robustness in practical design. This study evaluates the performance of the gaining-sharing knowledge-based algorithm (GSKA) through the optimization of three distinct steel frame design cases. These scenarios involve a more complex analysis of a 2-story, 1-bay steel moment frame incorporating geometric imperfections via the notional load method, designed under combined current and notional loading. The objective of optimization for all scenarios is to minimize the total structural weight while strictly adhering to the strength, stability and serviceability constraints of the (AISC LRFD, 2001) specification. The material properties remain consistent, with a modulus of elasticity of 200 GPa, a yield strength of 250 MPa, and a density of 7.85 ton/m³. This set of analyses aims to evaluate the effect of geometric imperfections on the three-dimensional steel frame design. Furthermore, this multi-problem framework provides a comprehensive basis for assessing the robustness and efficiency of the proposed GSKA-ETABS integrated methodology under both ideal and realistic design conditions.

6. Results and discussion

The minimum-weight optimum design of the steel space frame is successfully achieved. Adhering to the original study of the gaining-sharing knowledge-based algorithm (GSKA), the parameters P, k_f, k_r, and K were taken as 0.1, 0.5, 0.9, and 10, respectively. The mentioned parameters are taken from the reference study of Tunca (Tunca, 2025). The final results obtained by the GSKA employed here, along with those from the Harmony Search Algorithm (HSA) and the Genetic Algorithms (GAs) considered in the reference study, are presented comparatively in Table 1.

Table 1. Optimum final design of CASE-0

	GAs (Artar & Daloğlu, 2018)	HSA (Artar & Daloğlu, 2018)	GSKA (Tunca, 2025)
Group 1	W14 x 43	W16 x 36	W18 x 40
Group 2	W18 x 35	W18 x 35	W18 x 35
Group 3	W14 x 26	W14 x 34	W16 x 26
Minimum weight (kN)	37.68	37.36	36.52
No. of iter.	67	46	42

In terms of computational effort, GSKA required 42 iterations to converge, with each iteration comprising one structural analysis per candidate solution. The total number of analyses is 42 × population size (here, 30) = 1,260 analyses per case. Each analysis, including model update, solution, and results extraction via the ETABS OAPI, took approximately 9.5 seconds on average, resulting in a total runtime of roughly 3.25 hours per optimization case on a standard computer (Intel Core i3, 8GB RAM).

As can be seen comparatively in the Table 1, in terms of minimum weight, GSKA yielded a design that is 3.18% and 2.30% lighter than genetic algorithms (GAs) and harmony search algorithm (HSA), respectively. Furthermore, GSKA demonstrated the fastest convergence with 42 iterations, thereby enhancing computational efficiency. All design candidates complied with the constraints of the AISC-LRFD specification, without violation of the top story displacement, inter-story drift, axial force-bending moment interaction, and shear capacity limits.

The proposed GSKA-ETABS integrated framework was successfully applied to optimize the CASE-1 and CASE-2 steel frame scenarios described in the Problem Definitions section. Figure 2 illustrates the convergence history of the total structural weight across iterations for all three cases (CASE-0, CASE-1, CASE-2), demonstrating the algorithm's stable and efficient search capability.

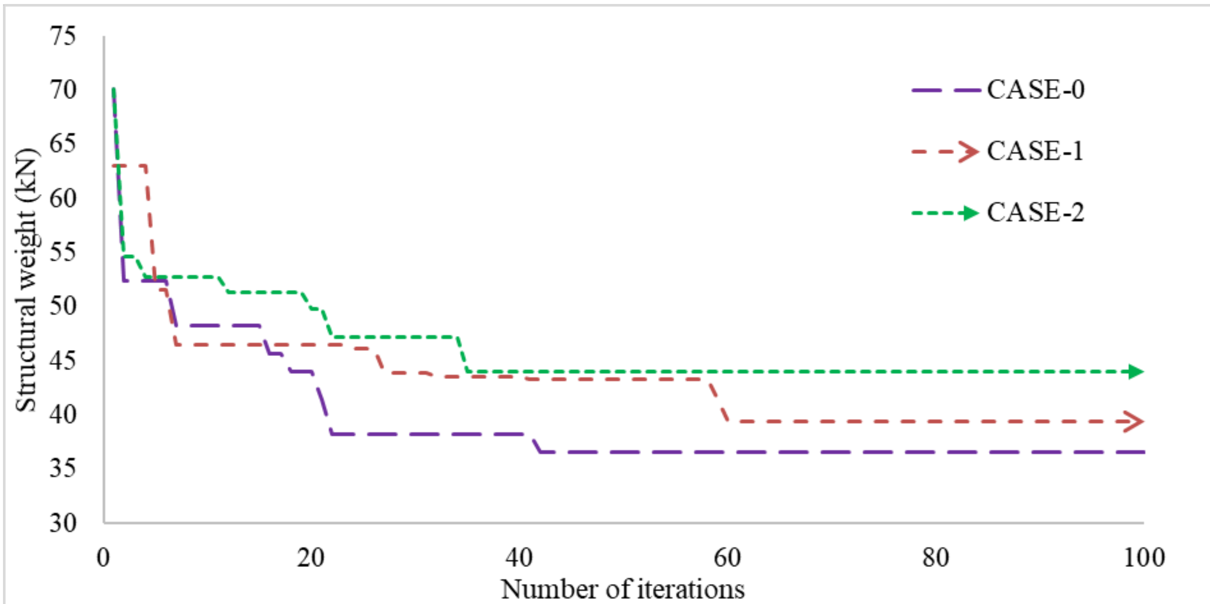

Figure 2. Optimization convergence for all cases.

Table 2 shows the optimal member sections identified for each scenario, while Figure 3 illustrates the final structural weights and compares these optimized space structures across the minimization process.

Table 2. Optimal design results for the three cases

	Best final sections	Min. weight (kN)
CASE-0 (Tunca, 2025)	W14x43, W18x35, W16x26	36.52
CASE-1	W21x50, W16x31, W12x26	39.37
CASE-2	W12x58, W18x40, W8x21	43.96

As summarized in Table 2 and Figure 3, the optimization results reveal a clear trend. For the 16-member frame without geometric imperfections (CASE-0), GSKA achieved a minimum structural weight of 36.54 kN using sections W14x43, W18x35, and W16x26 for groups 1, 2, and 3, respectively. When a notional load of 0.2% of story weight was introduced to model imperfections (CASE-1), the optimal weight increased to 39.37 kN, with heavier sections selected (W21x50, W16x31, W12x26). A further increase in the imperfection magnitude to 0.4% (CASE-2) resulted in a final weight of 43.96 kN, employing sections W12x58, W18x40, and W8x21. This nonlinear relationship highlights the significant impact of stability considerations driven by geometric imperfections on the final design. The increase in structural weight from CASE-0 to CASE-1 (7.80%) and CASE-2 (20.37%) can be attributed to the additional forces induced by the notional loads, which simulate the destabilizing effects of geometric imperfections. These notional loads amplify second-order (P-Delta) effects, leading to higher internal forces, particularly in columns subjected to combined axial and flexural demands. More importantly, the introduction of imperfections shifted the governing design constraint: in CASE-0, the design is controlled by the top drift limit, whereas in CASE-1 and CASE-2, member strength (PMM interaction) became the binding constraint. This shift necessitated the selection of larger sections to satisfy the more stringent strength requirements, resulting in the observed weight increases. In CASE-2, the substantial increase in column size (W12x58) stiffens the frame against lateral drift, allowing the orthogonal beams (Group 3) to be downsized to a lighter W8x21 section. This outcome reflects load redistribution: the heavier columns attract more lateral load, reducing the lateral demand on the beams and permitting them to be designed primarily for gravity loads and serviceability criteria. The optimization algorithm exploits this synergy to achieve overall weight minimization.

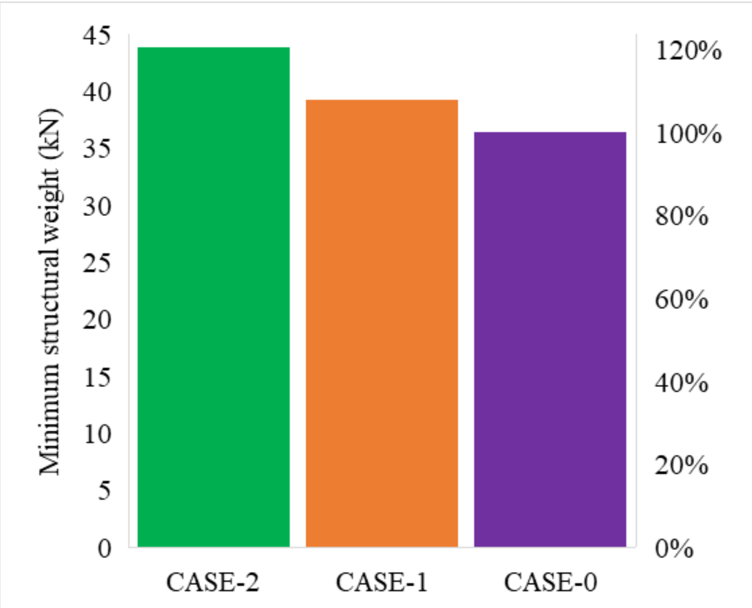

Figure 3. The comparison chart of minimum structural weight.

The structural integrity of all optimized designs is rigorously validated against AISC-LRFD constraints. As shown in the detailed constraint ratio outputs (e.g., PMM, shear, drift), all values remained below 0, confirming that no strength, stability, or serviceability limits are violated. For instance, the maximum PMM penalty is -0.397 for CASE-0, -0.068 for CASE-1, and -0.077 for CASE-2, all well within the safe limit. Similarly, the top drift and inter-story drift ratios were consistently below the prescribed code limits of 1.8 cm and 0.9 cm, respectively.

Table 3. Critical constraint checks ratios for optimal designs

	Max top drift	Max PMM	Max Vmaj	Max beam-column
	Eq. (3)	Eq. (7)	Eq. (6)	Eqs. (8-9)
CASE-0 (Tunca, 2025)	-0.072	-0.094	-0.840	-0.140
CASE-1	-0.140	-0.068	-0.714	-0.153
CASE-2	-0.465	-0.077	-0.612	-0.398

In Table 3, some critical constraint values are tabulated. The consistency of these validations across all scenarios underscores the reliability of the automated constraint-checking mechanism via the ETABS-OAPI.

Based on the constraint check ratios of the optimal designs, the governing performance limit shifts across the cases: CASE-0 is dominated by the max top drift constraint, whereas CASE-1 and CASE-2 are dominated by the max PMM ratio. This highlights a significant observation in structural optimization. The shift in the controlling constraint from top drift to member strength (PMM) as the case changes underscores the critical influence of geometric imperfections. By incorporating realistic imperfection patterns (as in CASE-1 and CASE-2), the optimization process reveals that member forces, rather than global displacements, can become the decisive design factor. This outcome emphasizes that neglecting geometric imperfections in optimal structural design can lead to non-conservative solutions, potentially underestimating the critical stresses within members. Therefore, accounting for geometric imperfections is essential for achieving a robust and safe optimum design. This shift from drift-controlled to strength-controlled design is not limited to moment frames. In other lateral-load-resisting systems such as eccentrically braced frames (EBFs) or concentrically braced frames (CBFs), geometric imperfections may similarly amplify axial and flexural demands, potentially making member strength or connection capacity the governing constraint. However, the degree of shift depends on the structural redundancy, stiffness distribution, and load paths.

Additionally, the distribution of optimum steel I-sections on a 16-element steel space frame, along with the demand capacity ratio (PMM) obtained from the finite element analysis, is shown in Figure 4.

7. Conclusions

This study presented and validated a fully automated structural optimization framework by synergistically integrating the gaining-sharing knowledge-based algorithm (GSKA) with the ETABS Open Application Programming Interface (OAPI). The methodology was demonstrated through the optimum design of three steel frame scenarios with varying degrees of geometric imperfection modeling. The key findings and contributions are as follows:

●Proven Algorithmic Performance: The GSKA demonstrated robust performance, efficiently navigating the discrete search space of standard steel sections. The convergence behavior shown in Figure 2 indicates effective balancing of exploration and exploitation, leading to satisfactory optimum solutions within a reasonable number of iterations for all three design problems.

●Significant Impact of Imperfections: The comparative results from Scenarios CASE-0, CASE-1, and CASE-2 quantitatively establish the critical influence of geometric imperfections on optimal steel design. The necessity to consider these imperfections, as simulated via notional loads, led to notably different optimal section selections and a non-linear change in structural weight, emphasizing their importance in practical, code-compliant design.

●Successful Automation & Integration: The core achievement of this study is the seamless, bidirectional integration between the metaheuristic optimizer and commercial FEA software. The Python-driven OAPI loop successfully automated model updating, analysis, design checking, and data retrieval, eliminating manual intervention and ensuring rigorous adherence to all AISC-LRFD constraints, as confirmed by the constraint ratio data.

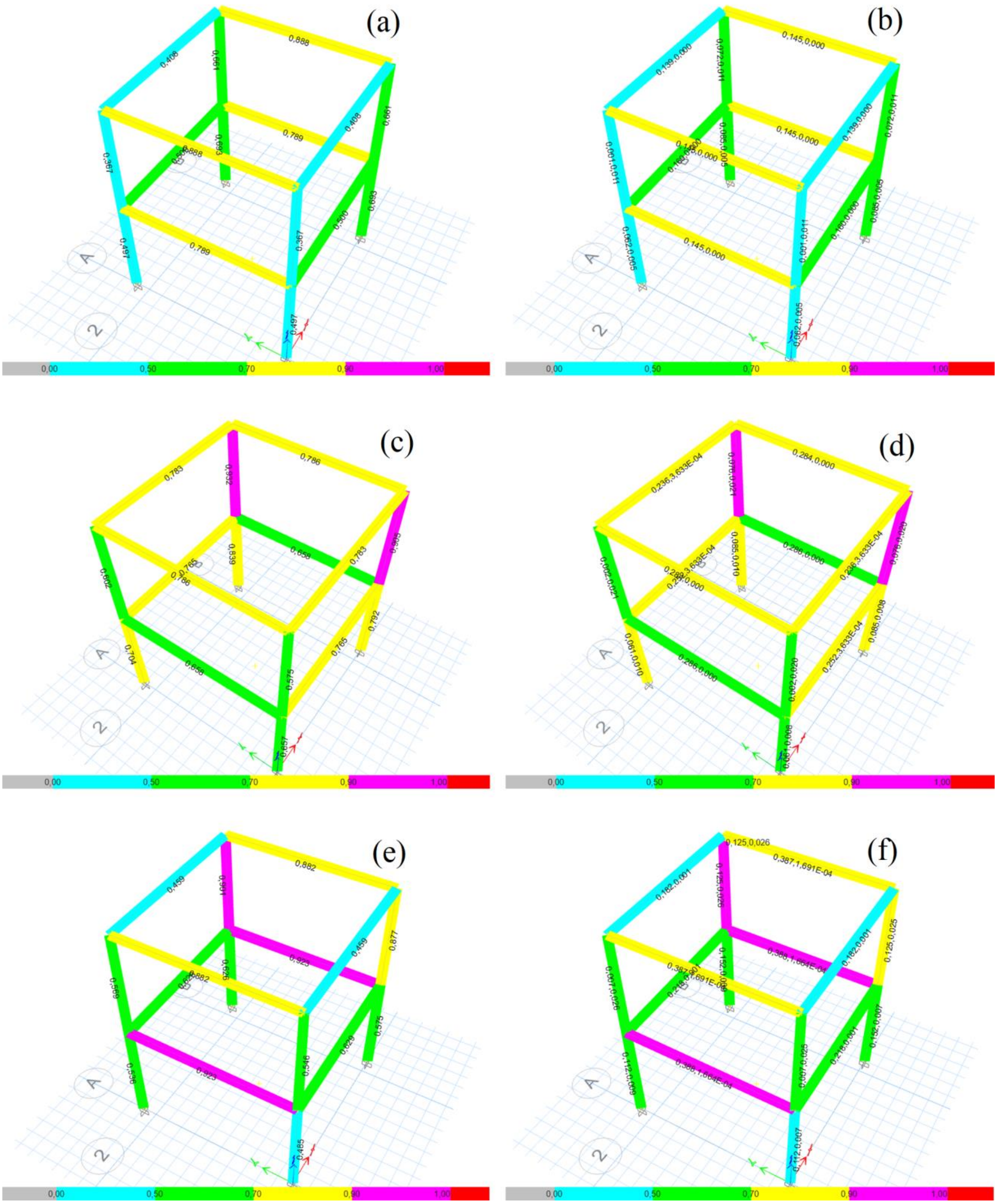

Figure 4. PMM and shear ratios of final designs. (a) PMM ratios for CASE-0. (b) Shear ratios for CASE-0. (c) PMM ratios for CASE-1. (d) Shear ratios for CASE-1. (e) PMM ratios for CASE-2. (f) Shear ratios for CASE-2.

●Practical Framework: The developed system provides a practical, reusable template for automating the design of complex steel structures. It offers tangible benefits in material efficiency, as seen in the optimized weights, and computational reliability by enforcing complete code compliance automatically.

In conclusion, the GSKA-ETABS synergy offers a powerful and efficient approach for the performance-based design optimization of steel frames. It bridges the gap between advanced metaheuristic search techniques and industry-standard analysis tools, paving the way for more reliable, economical, and automated structural design processes in engineering practice.

The findings of this study are directly applicable to the optimum design of low-to-mid-rise steel moment frames subjected to combined gravity and lateral loads, following AISC-LRFD specifications and using discrete standard sections. However, certain limitations must be noted. The current analyses are based on elastic second-order analysis, excluding material nonlinearity, inelastic buckling, or residual stresses. Furthermore, while the study focuses on a benchmark two-story, 16-member frame, the influence of geometric imperfections is expected to increase nonlinearly in taller or more flexible structures. Irregular geometries or complex lateral-load-resisting systems, such as eccentrically braced frames, may also exhibit different constraint-governing mechanisms. To address these constraints, future research will extend the framework to incorporate nonlinear analysis, alternative design codes (e.g., Eurocode), and multi-objective optimization addressing both cost and environmental impact. Additionally, future work will integrate the Effective Length Method alongside the Direct Analysis Method for a more comprehensive stability assessment.

Acknowledgement

The author would like to express their sincere gratitude to the editor and anonymous reviewers for their valuable comments and suggestions, which have significantly improved the quality and clarity of the manuscript.

Declaration of ethical code

The materials and methods used in this study do not require ethics committee approval and/or legal-special permission.

Conflicts of interest

The author declares that there is no conflict of interest.

References

AISC LRFD. (2001). *Manual of steel construction: Load and resistance factor design. American Institute of Steel Construction, Chicago* (AISC LRFD; Seismic Provisions for Structural Steel Buildings). American Institute of Steel Construction, Chicago, USA.

ANSI/AISC. (2022). *American Institute of Steel Construction. Supersedes the Seismic Provisions for Structural Steel Buildings, Chicago.*

Artar, M., & Daloğlu, A. T. (2018). Optimum weight design of steel space frames with semi-rigid connections using harmony search and genetic algorithms. *Neural Computing and Applications*, *29*(11), 1089–1100. https://doi.org/10.1007/s00521-016-2634-8

Aydogdu, I., Ormecioglu, T. O., Tunca, O., & Carbas, S. (2022). Design of large-scale real-size steel structures using various modified grasshopper optimization algorithms. *Neural Computing and Applications*, *34*(16), 13825–13848. https://doi.org/10.1007/s00521-022-07196-3

Bora, P., & Türkay, A. (2025). İki boyutlu ve 35 katlı betonarme bir perde-çerçeve sistemde diyagonal çelik çaprazların etkisinin araştırılması. *Gümüşhane Üniversitesi Fen Bilimleri Enstitüsü Dergisi*, *15*(4), 1222–1243. https://doi.org/10.17714/gumusfenbil.1779975

Chan, H. U., Walport, F., Slack, H., Wadee, M. A., & Gardner, L. (2025). Practical rules for defining initial geometric imperfections for in-plane stability design of steel frames. *Structures*, *82*, 110643. https://doi.org/10.1016/j.istruc.2025.110643

Erdem Çerçevik, A., Avşar, Ö., & Dilsiz, A. (2021). Optimal placement of viscous wall dampers in RC moment resisting frames using metaheuristic search methods. *Engineering Structures*, *249*, 113108. https://doi.org/10.1016/j.engstruct.2021.113108

ETABS. (2008). *Integrated finite element analysis and design of structures. Computers and Structures Inc, Berkeley.* [Computer software].

Li, Y.-P., & She, G.-L. (2025). Nonlinear dynamic response of graphene platelets reinforced cylindrical shells under moving loads considering initial geometric imperfection. *Engineering Structures*, *323*, 119241. https://doi.org/10.1016/j.engstruct.2024.119241

Mohamed, A. W., Hadi, A. A., & Mohamed, A. K. (2020). Gaining-sharing knowledge based algorithm for solving optimization problems: A novel nature-inspired algorithm. *International Journal of Machine Learning and Cybernetics*, *11*(7), 1501–1529. https://doi.org/10.1007/s13042-019-01053-x

Oğuzalp, Ş. N., Akkaya, S., & Eminoğlu, U. (2025). Güç sistemlerinde harmonik tespiti için gelişmiş meta sezgisel algoritmaların karşılaştırılması. *Gümüşhane Üniversitesi Fen Bilimleri Enstitüsü Dergisi*, *15*(2), 620–638. https://doi.org/10.17714/gumusfenbil.1618127

Prayogo, H., Yang, I.-T., & Cheng, M.-Y. (2024). Dynamic Gradient Boosted Metaheuristic approach for efficient reinforced concrete structure optimization. *Journal of Building Engineering*, *97*, 110864. https://doi.org/10.1016/j.jobe.2024.110864

Tunca, O. (2022). Design of buckling restrained steel braces using application programming interface between simulation and discrete optimization. *Structures*, *43*, 752–766. https://doi.org/10.1016/j.istruc.2022.07.010

Tunca, O. (2025, October 30). Bilgi Kazanım-Paylaşım Temelli Algoritma ile ETABS-OAPI destekli çelik yapı optimizasyonu. *Proceeding Book of 7th International Conference on Engineering and Applied Natural Sciences (ICEANS 2025), Konya-Türkiye.* 7th International Conference on Engineering and Applied Natural Sciences (ICEANS 2025). https://www.iceans.org/

Tunca, O., & Carbas, S. (2024). Sustainable and cost-efficient design optimization of rectangular and circular-sectioned reinforced concrete columns considering slenderness and eccentricity. *Structures*, *61*, 105989. https://doi.org/10.1016/j.istruc.2024.105989

Tunca, O., & Carbas, S. (2026). Human-Inspired Optimization Algorithms for Cost Minimization in Reinforced Concrete Column Design. In G. Bekdaş & S. M. Nigdeli (Eds.), *Artificial Intelligence in Civil Engineering* (Vol. 643, pp. 63–92). Springer Nature Switzerland. https://doi.org/10.1007/978-3-032-07738-7_4

Zekavati, A., Abedi, K., Chenaghlou, M. R., & Charkhtab Basim, M. (2025). A proposed approach for failure analysis of lattice transmission towers considering geometric imperfection effects. *Engineering Failure Analysis*, *168*, 109068. https://doi.org/10.1016/j.engfailanal.2024.109068